Environmental Science & Technology

Article

pubs.acs.org/est

Photochemical Transformation of Carboxylated Multiwalled Carbon Nanotubes: Role of Reactive Oxygen Species

Xiaolei Qu, Pedro J. J. Alvarez, and Qilin Li*

Department of Civil and Environmental Engineering, Rice University, Houston, Texas 77005, United States

Supporting Information

ABSTRACT: The study investigated the photochemical transformation of carboxylated multiwalled carbon nanotubes (COOH-MWCNTs), an important environmental process affecting their physicochemical characteristics and hence fate and transport. UVA irradiation removed carboxyl groups from COOH-MWCNT surface while creating other oxygen-containing functional groups with an overall decrease in total surface oxygen content. This was attributed to reactions with photogenerated reactive oxygen species (ROS). COOH-MWCNTs generated singlet oxygen ($^1O_2$) and hydroxyl radical ($^\bullet OH$) under UVA light, which exhibited different reactivity toward the COOH-MWCNT surface. Inhibition experiments that isolate the effects of $^\bullet OH$ and $^1O_2$ as well as experiments using externally generated $^\bullet OH$ and $^1O_2$ separately revealed that $^\bullet OH$ played an important role in the photochemical transformation of COOH-MWCNTs under UVA irradiation. The Raman spectroscopy and surface functional group analysis results suggested that $^\bullet OH$ initially reacted with the surface carboxylated carbonaceous fragments, resulting in their degradation or exfoliation. Further reaction between $^\bullet OH$ and the graphitic sidewall led to formation of defects including functional groups and vacancies. These reactions reduced the surface potential and colloidal stability of COOH-MWCNTs, and are expected to reduce their mobility in aquatic systems.

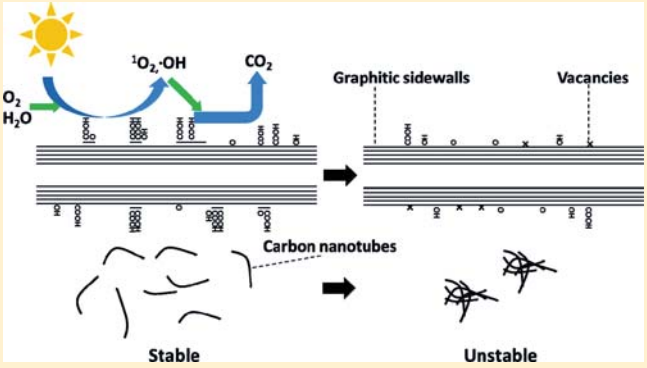

INTRODUCTION

The remarkable electronic, mechanical, and optical properties of carbon nanotubes (CNTs) have enabled a wide range of promising applications.[1] The annual production of CNTs in the United States has exceeded 2000 tons in 2011.[1] The fast growing production and potential widespread use in consumer and industrial products (e.g., electronics, composite materials, and sporting equipment) may result in significant environmental exposure and calls for careful assessment of their potential risk to human health and ecosystems. The fate, transport, and toxicity of CNTs need to be carefully studied to assist risk assessment as well as mitigate potential hazards.

Environmental transformation of CNTs could lead to changes in their physicochemical properties that govern their mobility and toxicity. Several studies have investigated the potential routes of CNT transformation or degradation under natural conditions, most of which focus on enzyme-catalyzed degradation processes.[2−4] Peroxidase enzymes, mainly horseradish peroxidase and myeloperoxidase, were reported to degrade single-walled carbon nanotubes (SWCNTs) and multiwalled carbon nanotubes (MWCNTs) in the presence of trace amount of H_2O_2.[3,4] The degradation was attributed to the high oxidative potential of peroxidases and their byproducts such as hypochlorite.[2] However little is known about the abiotic transformation of CNTs in the environment. Our recent study reported that COOH-MWCNTs lost surface oxygen-containing functional groups under UVA irradiation in aqueous solutions.[5] Many carbon based nanomaterials including fullerenes, graphene oxides, and carbon nanotubes possess unique photochemical properties. Fullerene nanoparticles are able to generate $^1O_2$ through energy transfer within solar spectrum, which in turn oxidizes fullerene molecules, resulting in water-soluble fullerene derivatives and eventually mineralization.[6−11] Graphene oxide behaves similar to a semiconductor photocatalyst under UV light, generating electron−hole pairs which leads to graphene oxide with less oxygen content and CO_2 and H_2 evolution.[12] Certain CNTs (e.g., carboxylated SWCNT and MWCNT) were found to produce ROS when exposed to UVA light or near-infrared light.[5,13,14] ROS have similar or higher oxidative potential than the oxidants involved in the enzyme-catalyzed degradation processes and are produced right on the CNT sidewall, where they have easy access to reactive sites. We hypothesize that COOH-MWCNTs will undergo photochemical transformation under solar irradiation by reacting with self-generated ROS, and such transformation will lead to changes in their physicochemical characteristics and consequently fate and transport in the environment.

Received: July 25, 2013
Revised: November 15, 2013
Accepted: November 20, 2013
Published: November 20, 2013

dx.doi.org/10.1021/es4033056 | Environ. Sci. Technol. 2013, 47, 14080−14088

In this study, we examined our hypothesis and investigated mechanisms of the photochemical transformation of COOH-MWCNTs under UVA light, the major UV component in sunlight. ROS generation by COOH-MWCNTs under UVA light was quantified using probe molecules, and their respective impacts on COOH-MWCNT surface chemistry and colloidal stability were examined using individual, externally generated ROS. Experimental data showed strong evidence that self-generated ROS played critical roles in the photochemical transformation of COOH-MWCNTs under UVA irradiation, which led to reduction in surface oxygen mainly through removal of carboxyl groups. Such transformation reduced the surface potential and consequently colloidal stability of COOH-MWCNTs, suggesting reduced mobility in the aquatic environment.

MATERIALS AND METHODS

Materials. COOH-MWCNTs (>95%, PD15L1-5-COOH) were purchased from NanoLab, Inc. (Newton, MA) with reported diameter and length to be 15 ± 5 nm and 1−5 μm, respectively. They were produced by refluxing pristine MWCNTs synthesized by chemical vapor deposition in a concentrated HNO_3/H_2SO_4 mixture. Terephthalic acid (TPA, >99%) was purchased from Acros Organics (New Jersey, U.S.A.). Furfuryl alcohol (FFA, 98%), 2,3-bis(2-methoxy-4-nitro-5-sulfophenyl)-2*H*-tetrazolium-5-carboxanilide (XTT, >90%), 2-hydroxyterephthalic acid (HTPA, 97%), Rose Bengal (95%), 2,2,2-trifluoroacetic anhydride (TFAA, >99%), 2,2,2-trifluoroethanol (TFE, >99%), *N*,*N*′-di-*tert*-butyl-carbodiimide (DTBC, >99%), and 2,2,2-trifluoroethylhydrazine (TFH, 70 wt. % solution in water) were purchased from Aldrich Chemicals (Milwaukee, WI). All other chemicals were reagent grade. Deionized water (18.2 MΩ·cm resistivity at 25 °C) was produced by a Barnstead Epure water purification system (Dubuque, IA).

Preparation of COOH-MWCNT Stock Suspension. The aqueous COOH-MWCNT stock suspension was prepared by direct sonication. Forty milligrams of COOH-MWCNT was added to 400 mL deionized water in a 500-mL glass beaker. The mixture was placed in an ice bath and sonicated with a sonicating probe (Vibra-Cell VCX 500, Sonics & Material, Newtown, CT) at 100 W for 30 min. A stable suspension was obtained after sonication and was stored in dark at room temperature until use.

Photochemical Reaction Experiments. Photochemical reaction experiments were carried out in a Luzchem LZC-4 V Photoreactor (Luzchem, Ottawa, Ontario, Canada). Eight 8W black-light lamps (EIKO F8T5/BL, 4 on each side) with an emitting spectrum in the UVA range (centered at 350 nm) were employed to mimic the UVA fraction of the solar spectrum. The total light intensity at the center of the reactor where the sample suspension was located was measured to be 2.4 mW/cm^2 using a radiometer (Control Company, Friendswood, TX). This intensity is comparable to the UVA intensity of sunlight measured at the ground level on a sunny day in Houston, Texas. In most experiments, a 500-mL glass beaker containing 400 mL of 10 mg/L COOH-MWCNTs with unadjusted pH (5.7 ± 0.3) was placed at the center of the photoreactor and exposed to the irradiation for predetermined periods of time. For experiments under anoxic conditions, 100 mL COOH-MWCNT suspension (10 mg/L) in a 150-mL glass bottle was purged with N_2 for 1 h and sealed before irradiation. A parallel sample without N_2 purge was irradiated in a 150-mL glass bottle with the cap open. The dissolved oxygen (DO) concentration in the suspension was measured by a dissolved oxygen meter (YSI 550A, YSI Incorporated). After irradiation, the CNTs in the suspension were collected by filtering the suspension through a 0.1-μm PVDF membrane (Millipore, Billerica, MA). The CNTs retained on the membrane were thoroughly washed with deionized water. In the L-histidine inhibition experiment, CNTs were washed with 100 mL deionized water for 3 times and 100 mL methanol for 8 times (Supporting Information Figure S1). Samples were dried in vacuum at 80 °C for 24 h before further analysis.

ROS Measurements. Production of $^1O_2$, O_2^-, and $^\bullet$OH was characterized using respective ROS probes under the same irradiation conditions used in the photochemical reaction experiments. 100 mL suspension of 10 mg/L COOH-MWCNTs with the respective ROS probe was covered with vented parafilm, stirred, and irradiated by UVA light at ∼2.4 mW/cm^2 provided by six 4W black-light lamps (EIKO F4T5/BL, centered at 350 nm, three on each side) in a custom-made photoreactor. Sample aliquots of 5 mL were withdrawn at predetermined times and filtered through 0.2-μm pore size PTFE syringe filters (Millipore, Billerica, MA) before analysis of the remaining probe compound or reaction product. For $^\bullet$OH analysis, samples were filtered through 30 K MWCO centrifugal filters (Amicon Ultra, Millipore, Massachusetts) because the measurement was highly sensitive to remaining CNTs and fragments even at trace amount. Before sampling, deionized water was added to compensate the volume loss due to evaporation. Blank experiments were run using solutions containing only the ROS probes under the same irradiation conditions described above; dark control experiments were also performed for each CNT/ROS probe combination.

FFA, XTT, and TPA were used as probes for $^1O_2$, O_2^-, and $^\bullet$OH, respectively. $^1O_2$ generation was quantified by the loss of FFA[15] added at an initial concentration of around 0.2 mM. At this concentration, FAA is specific to $^1O_2$.[16,17] The remaining FFA in the filtered samples was analyzed by an HPLC (SHIMADZU, Japan) equipped with a C18 column (Ecilipse XD8, Agilent) and a UV detector at 218 nm. The mobile phase comprised 30% acetonitrile and 70% 0.1 wt % phosphoric acid and was run at 0.5 mL/min.

O_2^- production was determined by the generation of XTT formazan at an XTT initial concentration of 0.05 mM.[13,18] The 0.05 mM XTT solution was filtered through 0.45-μm membrane before use. The formation of XTT formazan was monitored using a SHIMADZU UV−vis spectrophotometer at 470 nm.

The production of $^\bullet$OH was characterized using a fluorescence probe, TPA.[19,20] TPA was dissolved in 2 mM NaOH, stirred for 24 h, filtered through a 0.45-μm membrane, and added to the COOH-MWCNT suspension at 458 μM. The reaction between $^\bullet$OH and TPA produces HTPA, which was analyzed by fluorescence spectroscopy (HITACHI F-2500, Japan) with excitation and emission wavelengths of 315 and 425 nm, respectively.

Reactions with Externally Generated ROS. As shown later, the COOH-MWCNTs generate more than one ROS under UVA irradiation, but at very low concentrations. To study the reactions between COOH-MWCNTs and individual ROS within a reasonable time frame, external ROS sources were used. $^\bullet$OH was generated by UV photolysis of H_2O_2. 50 mL 100 mg/L COOH-MWCNTs was mixed with 50 mL 30% H_2O_2 in a 150-mL glass beaker and exposed to UVA irradiation

at 2.0 mW/cm^2 in the Luzchem LZC-4 V Photoreactor. After predetermined time, the suspension was filtered through a 0.1-μm membrane, and CNTs were collected, washed with deionized water, and dried in vacuum at 80 °C for 24 h before further analysis.

$^1O_2$ was produced by photosensitizing Rose Bengal using visible light from eight fluorescence lamps (SYLVANIA F8T5/CW) in the Luzchem LZC-4 V Photoreactor. Oxygen was continuously added into the solution containing 50 mg/L COOH-MWCNTs and 12.5 μM Rose Bengal. After predetermined reaction time, the CNTs were collected by filtering the suspension through a 0.1-μm membrane, and washed with 100 mL methanol for 6 times to remove adsorbed Rose Bengal. The samples were further washed with deionized water and dried in vacuum at 80 °C for 24 h before analysis.

Characterization of COOH-MWCNTs. The surface chemical composition of CNTs was characterized using X-ray photoelectron spectroscopy (XPS). XPS analyses were carried out using a PHI Quanteria SXM scanning X-ray microprobe ULVAC-PHI with a 24.8 W X-ray source and a 200.0 μm X-ray spot size at 45.0° (26.00 eV). The atomic concentrations of different elements were quantified by the areas of corresponding photoelectron peaks. The concentrations of three major oxygen-containing functional groups including carboxyl, hydroxyl and carbonyl were quantified using a chemical derivatization method in conjunction with XPS.[21,22] Functional groups were quantified one at a time. The recipes of derivation reagents were as follow: 1.0 mL TFE, 0.4 mL pyridine and 0.2 mL DTBC for carboxyl groups; 1.0 mL TFAA for hydroxyl groups; and 0.4 mL TFH for carbonyl groups. Briefly, a piece of CNT cake layer was placed in a 1.5 mL microcentrifuge tube with cap removed. The derivation reagents for a specific functional group were added into a glass reaction vessel (Supporting Information Figure S2) and put in liquid nitrogen. After the reagents were completely frozen, the reaction vessel was withdrawn from the liquid nitrogen. The microtube containing the CNT sample was immediately put into the reaction vessel, which was evacuated using a vacuum pump and sealed. The derivatization reaction was allowed to proceed for 24 h at room temperature, and the samples were analyzed immediately by XPS. The atomic oxygen concentrations in major oxygen-containing functional groups including carboxyl, hydroxyl, and carbonyl was calculated from the C(1s), F(1s), and N(1s) contents after derivatization and the surface carbon concentration prior to derivatization. Oxygen associated with other functional groups, termed residue oxygen, was calculated from the difference between the total surface oxygen concentration and that associated with the three major oxygen-containing functional groups.

Raman spectra of CNT samples were acquired using a RENISHAW in Via Raman microscope (RENISHAW, Hoffman Estates, IL) with a 514 nm laser focused through a 50× objective lens. Each sample was scanned 10 times. The hydrodynamic diameter of CNTs were measured five times at 23 °C by dynamic light scattering (DLS) using a Zen 3600 Zetasizer Nano (Malvern, Worcestershire, U.K.). The ζ potential of CNTs in 1 mM NaCl solution was measured in folded capillary cells (Malvern, Worcestershire, U.K.) by phase analysis light scattering (PALS) at 23 °C. Ten measurements were carried out for each sample.

Sedimentation Experiments. Sedimentation experiments were conducted to characterize COOH-MWCNT colloidal stability before and after reaction. Immediately before sedimentation experiments, COOH-MWCNT samples were resuspended in deionized water using a sonication cup horn (Sonics & Material, Newtown, CT) at 100 W for 5 min. The ionic strength of the suspension was adjusted to 10 mM using NaCl to induce aggregation and sedimentation. Sedimentation kinetics was characterized by monitoring light absorbance at 350 nm as a function of time using a SHIMADZU UV−vis spectrometer.

RESULTS AND DISCUSSION

Changes in COOH-MWCNT Surface Chemistry under UVA Irradiation. The hydrodynamic diameter of COOH-MWCNTs in deionized water was 236 ± 4 nm, close to the value reported in our previous study using the same preparation method.[23] The total surface oxygen concentration of COOH-MWCNTs (O[Total]) before and after exposure to UVA light is compared in Figure 1. UVA irradiation reduced the O[Total]

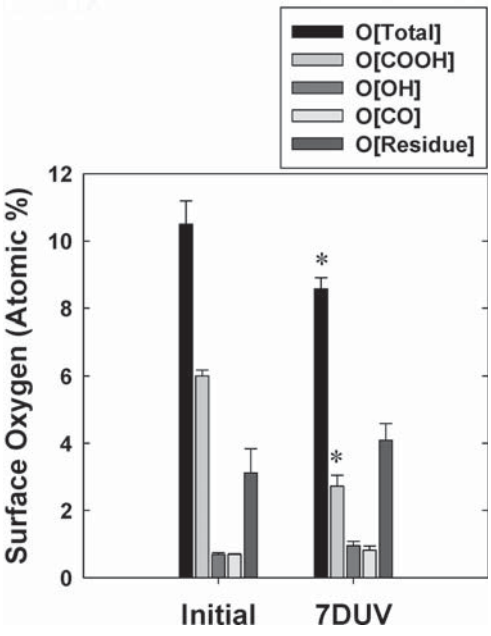

Figure 1. Surface oxygen (atomic %) and its composition on the initial and 7-day UVA-irradiated (7DUV) COOH-MWCNT surfaces. Error bars represent standard deviation. Star signs (*) denote statistically significant difference ($p < 0.05$, t-test) from the initial condition.

from 10.50 ± 0.69% to 8.58 ± 0.33% in 7 days. The decrease in O[Total] after UVA irradiation agrees with our earlier study.[23] In the meantime, oxygen associated with carboxyl groups, O[COOH], decreased from 6.00 ± 0.17% to 2.72 ± 0.32%, while O[OH] and O[CO] increased slightly and the residue oxygen (O[Residue]) increased from 3.12 ± 0.72% to 4.09 ± 0.50%. Changes of COOH-MWCNT surface functionality during UVA irradiation were previous studied by deconvolving XPS C(1s) spectra.[23] The C(1s) spectra of the initial and 7-day irradiated COOH-MWCNT samples were deconvolved into three peaks, representing underivatized, mono-oxygenated carbon, and dioxygenated carbon. The percentage of dioxygenated carbon (C═O and O−C−O) was significantly reduced by UVA irradiation, while mono-oxygenated (C−O) and underivatized carbon slightly increased, consistent with our results (Figure 1). While decarboxylation of COOH-MWCNTs was suggested in this earlier study,[5] the current study provides direct evidence.

ROS Production by COOH-MWCNTs. Our results show that COOH-MWCNTs generated notable amount of $^1O_2$ and $^\bullet OH$, but little O_2^- during UVA irradiation (Figure 2). No significant amount of XTT formazan was generated during 69 h of UVA irradiation (data not shown), suggesting little O_2^- production.

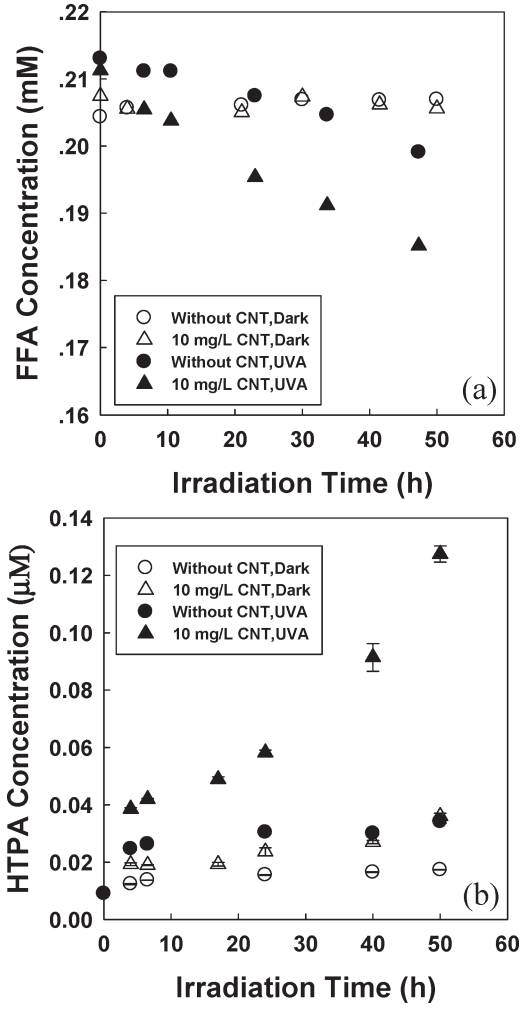

Figure 2. FFA loss, representing $^1O_2$ generation (a), and HTPA generation, representing $^\bullet OH$ generation (b) as a function of irradiation time with and without the presence of 10 mg/L COOH-MWCNTs and UVA light. Error bars represent standard deviation.

Figure 2a presents FFA concentration as a function of reaction time. In dark conditions, FFA, the $^1O_2$ probe, was stable both with and without COOH-MWCNTs. In the absence of COOH-MWCNTs, 6.6% FFA was lost after 47.3 h irradiation due to volatilization. FAA degradation was much faster in the presence of 10 mg/L COOH-MWCNTs, with a 12.4% loss in the same time period, suggesting production of $^1O_2$ by the CNTs. After adjusted for volatilization using the UVA irradiated FFA control data, the pseudosteady-state concentration, $[^1O_2]_{ss}$, was calculated to be 2.31×10^{-15} M. This value is comparable to $[^1O_2]_{ss}$ generated by carboxylated and polyethylene glycol functionalized SWCNTs (3.3×10^{-14} and 1.46×10^{-14} M, respectively) exposed to a UVA light at higher intensity.[13]

The production of HTPA from reaction of TPA with $^\bullet OH$ is shown in Figure 2b. In dark conditions, small amount of HTPA was formed, indicating that COOH-MWCNTs might be able to oxidize TPA without photoexcitation. During UVA irradiation, the HTPA concentration increased with increasing irradiation time in the presence of COOH-MWCNTs, while little HTPA was formed in the absence, indicating photogeneration of $^\bullet OH$ by COOH-MWCNTs. The pseudosteady-state concentration $[^\bullet OH]_{ss}$, was calculated to be 2.00×10^{-19} M, much lower than previous reported for carboxylated SWCNTs (1.58×10^{-15} M) exposed to a UVA light at higher intensity.[13]

It is worth noting that the actual ROS production by COOH-MWCNTs is difficult to quantify due to the micro-heterogeneous distribution of ROS in solutions.[24,25] The short lifetime of $^1O_2$ and $^\bullet OH$ (~4 μs and ~nanoseconds in water, respectively[26,27]) leads to very limited diffusion length. Thus a steep ROS concentration gradient is expected from the CNT surface to the bulk solution. Earlier studied have reported that the $^1O_2$ concentration inside and near the irradiated humic acid macromolecules was 2−3 orders of magnitude higher than the value measured in the bulk aqueous phase using FFA.[24,28] As a result, the ROS could have much greater impact on CNT surface chemistry than that expected based on the measured bulk concentrations as they were generated and consumed right on the CNT surface. The photoactivity of CNTs was also reported to depend on their surface functionality and defects.[13] Unfunctionalized CNTs were found to exhibit no ROS production under UVA light; while carboxylated and polyethylene glycol functionalized CNTs were both photoactive.[13,14] Therefore, loss of surface oxygen-containing groups during UVA irradiation may gradually reduce the photoactivity of the nanotubes.

Inhibition Experiments. To further reveal the reaction mechanisms, three sets of inhibition experiments were conducted and the results are summarized in Figure 3. In the first experiment, L-histidine was used to scavenge both $^1O_2$ and $^\bullet OH$.[29] In the presence of 10 mM L-histidine, there was no

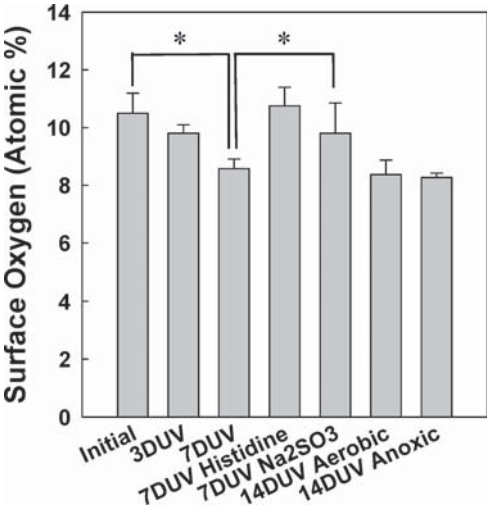

Figure 3. Surface oxygen (atomic %, O[Total]) of COOH-MWCNTs before and after UVA irradiation in deionized water (3DUV, 7DUV), 10 mM L-histidine (7DUV Histidine) or Na_2SO_3 (7DUV Na_2SO_3), and under aerobic (14DUV Aerobic) or anoxic (14DUV Anoxic) conditions. Note that the 14DUV Aerobic and 14DUV Anoxic samples were irradiated in glass containers different from other samples which attenuate more UVA light. Error bars represent standard deviation. Star signs (*) denote statistically significant difference between linked data points ($p < 0.05$, t-test).

significant change in O[Total] after 7 days of irradiation, suggesting that $^1O_2$ and/or •OH played an important role in the photochemical transformation of the COOH-MWCNTs. The irradiation was also carried out under anoxic conditions (DO = 0.68 mg/L). Because $^1O_2$ is reported to be produced by a type II photosensitization reaction where the photoexcited CNTs transfer energy to dissolved O_2,[13] its production is expected to be suppressed in anoxic condition. A previous study showed that phototransformation of fullerene nanoparticles was inhibited in anoxic condition due to limited $^1O_2$ formation.[10] However, O[Total] after 14 days of UVA irradiation, 8.37 ± 0.50%, was similar to that after a parallel experiment under aerobic conditions (DO = 5.33 mg/L). The result suggested that reaction with $^1O_2$ was not an important mechanism for the photochemical transformation of COOH-MWCNTs. On the other hand, •OH is reported to be photogenerated through either reactions between oxidized carbon nanotubes and water or electron transfer to molecular oxygen.[13,14] The similar phototransformation in aerobic and anoxic conditions suggest that the latter is not an important pathway. UV excited SWCNTs were previously suggested to be able to react with water to yield •OH.[30] It is possible that COOH-MWCNTs may photogenerate •OH through the same pathway. Another possible mechanism is that highly oxidized CNT sidewall fragments possess photoactivity similar to graphene oxide, which can be excited by UVA light to generate electron−hole pairs.[12] The electron holes can either directly react with COOH-MWCNTs or form •OH with water, both leading to the oxidation of COOH-MWCNTs. Significant mineralization of COOH-MWCNTs was detected during UVA irradiation (Supporting Information Figure S3), consistent with the oxidation process induced by ROS. Irradiation experiments were further carried out in the presence of an electron hole and •OH scavenger, Na_2SO_3.[31,32] As shown in Figure 3, the COOH-MWCNT phototransformation was inhibited by 10 mM Na_2SO_3, consistent with the hypothesized role of electron holes and/or •OH in photochemical transformation of COOH-MWCNTs. However, the relative contribution of each mechanism requires further investigation.

Reactions of $^1O_2$ and •OH with COOH-MWCNTs. To better isolate the effects of $^1O_2$ and •OH and to accelerate the reactions, external sources of $^1O_2$ and •OH were used to react with COOH-MWCNTs.

Rose Bengal was excited by visible light to produce $^1O_2$ at a steady state concentration of 7.27×10^{-12} M. As shown in Figure 4, there was notable increase in O[OH], O[CO] and O[Residue] on the COOH-MWCNT surface, while O-[COOH] decreased from 6.00 ± 0.17% to 3.94 ± 0.31% after 3 days of reaction. These trends agree with the corresponding changes in surface functional groups during the photo reaction experiment. The increase in O[OH], O[CO] and O[Residue] is also consistent with previous experimental studies and density functional theory calculations, which showed that $^1O_2$ can oxidize pristine SWCNT to produce surface oxides such as cycloaddition and epoxy structures.[30,33,34] However, the O[Total] of COOH-MWCNTs had no significant change after reactions with $^1O_2$. This shows that $^1O_2$ contributes to both surface oxide formation and decarboxylation.

•OH was generated by direct photolysis of H_2O_2 with a UVA source, and the $[•OH]_{ss}$ was measured to be the 5.53×10^{-16} M. Compared to this high external $[•OH]_{ss}$, the impact of ROS generated by COOH-MWCNTs was expected to be negligible.

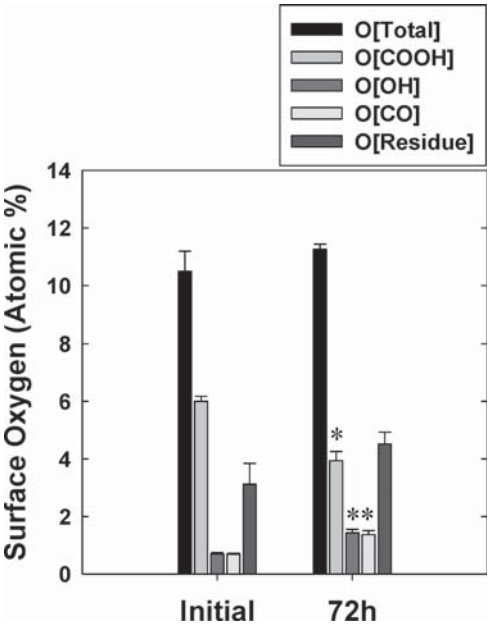

Figure 4. Surface oxygen (atomic %) and its composition on the original and 72 h $^1O_2$-treated COOH-MWCNTs surfaces. Error bars represent standard deviation. Star signs (*) denote statistically significant difference ($p < 0.05$, t-test) from the initial condition.

The O[Total] and the distribution of major oxygen-containing functional groups after reacting with •OH are presented in Figure 5. The O[total] decreased gradually with increasing reaction time and reached a plateau at ∼5% O after 11 h. Reactions between MWCNTs and H_2O_2 in dark had much less influence on the CNT surface oxygen content as H_2O_2 was a much weaker oxidant than •OH (Figure 5a). To rule out the possibility that the plateau was due to H_2O_2 depletion, another experiment was performed (denoted as pentagram in Figure 5a) in which COOH-MWCNTs were harvested after 16.5 h, resuspended in a fresh 15% H_2O_2 solution and reacted for another 7.5 h. The O[total] measured (4.90 ± 0.14%) was similar to that measured without H_2O_2 replenishment, suggesting the plateau was not caused by H_2O_2 depletion. The oxygen-containing functional groups have different reactivity toward •OH depending on their nature and location. However, given the high oxidative potential of •OH (E_0 = 2.3 V),[35] it is unlikely that these oxygen-containing groups (∼ 5% O) are inert to •OH. Reactions with •OH are hypothesized to both add (by oxidizing carbon) and remove (by decarboxylation) oxygen as shown in eqs 1−4.[36,37]

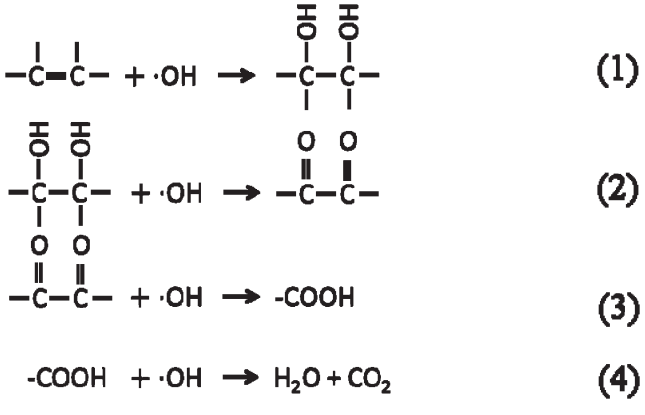

dx.doi.org/10.1021/es4033056 | Environ. Sci. Technol. 2013, 47, 14080−14088

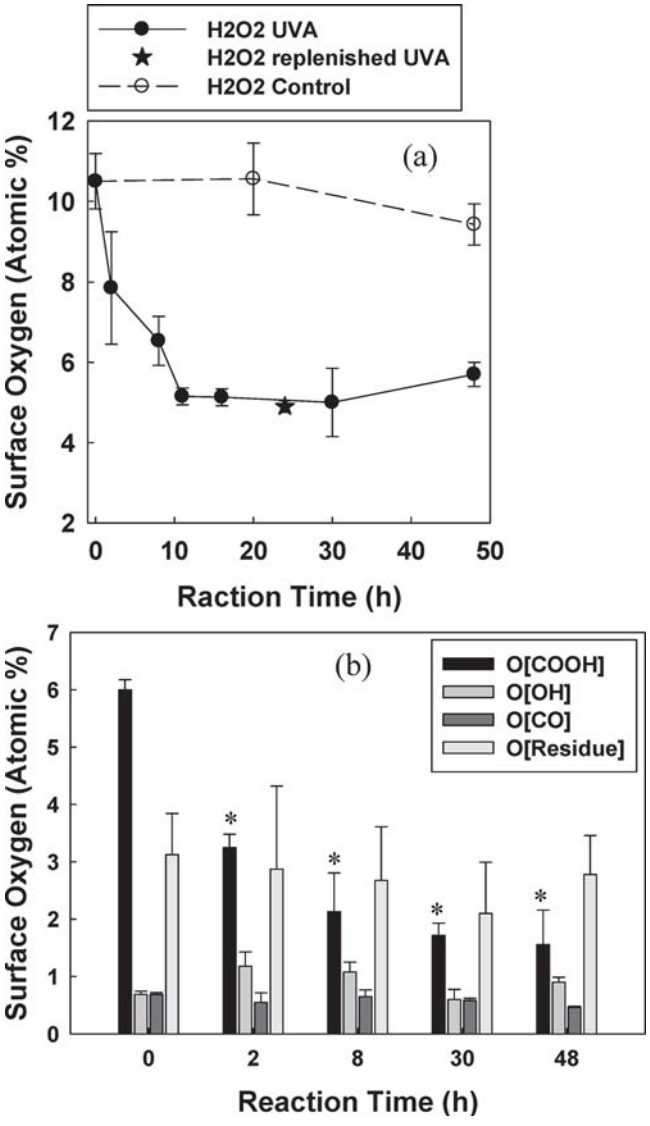

Figure 5. Surface oxygen (atomic %) (a) and the distribution of major oxygen-containing functional groups (b) on initial and •OH-treated COOH-MWCNTs surfaces as a function of reaction time with •OH. Error bars represent standard deviation. Each reaction time represents an independent experiment. Star signs (*) denote statistically significant difference ($p < 0.05$, t-test) from the initial condition.

The •OH can oxidize graphitic carbon to generate oxygen-containing functional groups (eqs 1−3); meanwhile it also can remove carboxyl groups and generate CO_2, as supported by the observed mineralization of COOH-MWCNTs under UVA light (Supporting Information Figure S3). We speculate that this dynamic process reached equilibrium after 11 h at around 5% O. Figure 5b shows that COOH-MWCNTs continuously lost carboxyl groups upon reaction with •OH, while concentrations of other oxygen-containing functional groups have no distinguishable trend.

The changes in COOH-MWCNT surface structure was studied by Raman spectroscopy. COOH-MWCNTs have three characteristic modes: the radial breathing mode, the tangential mode (G-band (~1585 cm^{-1})) and the D mode (~1353 cm^{-1}). The D mode is the most studied feature, and its intensity is commonly associated with defects or amorphous carbon.[38,39] The G-band, on the other hand, is typically associated with well-ordered sp^2 carbon on the graphitic sidewall. The intensity ratio of these two bands, I_D/I_G, was suggested to be a sensitive indicator for the abundance of defects.[40] The I_D/I_G of COOH-MWCNTs slightly increased from 0.915 to 0.921 after 72 h of reactions with $^1O_2$. This is consistent with the finding that reactions with $^1O_2$ introduced oxygen-containing functional groups, resulting in more defects. Interestingly, the I_D/I_G value sharply decreased from 0.915 to 0.779 in the first 2 h of reaction with •OH and increased afterward (Figure 6). Such nonmonotonic change of I_D/I_G value was also observed in enzyme-catalyzed degradation of oxidized MWCNTs and was attributed to the exfoliation of highly oxidized graphitic lattice from the nanotube surface.[4] The COOH-MWCNTs used in this study is modified from pristine MWCNTs by sulfuric/nitric acids treatment. It has been reported that a large portion of the carboxyl groups created by acid treatment is on carboxylated carbonaceous fragments (CCF) on the nanotube surface.[39] We speculate that the initial decrease of I_D/I_G and O[COOH] is caused by the degradation or exfoliation of CCF, which is known to lower the D-band intensity as the inner graphitic sidewall is exposed.[39] The following increase of I_D/I_G is attributed to the formation of defects (e.g., functional groups and vacancies) on the graphitic sidewall, which has been observed in many studies when pristine CNTs underwent surface oxidation.[36,37,41,42] The I_D/I_G continued to rise after 11 h of reaction when the surface oxygen remained constant, suggesting formation of new oxygen containing functional groups and vacancies (from decarboxylation), which may eventually lead to the degradation of the CNT structure.

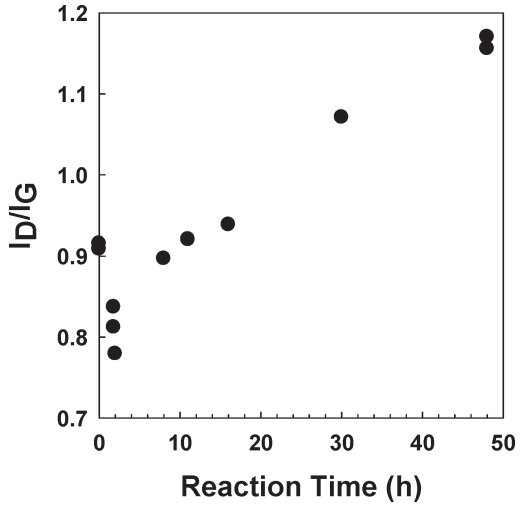

Figure 6. Intensity ratio of the D mode and the G mode of COOH-MWCNT Raman spectra, I_D/I_G, as a function of reaction time with •OH.

Impact of OH on the Stability of COOH-MWCNTs. Our previous study found that UVA irradiation reduced the negative surface potential and colloidal stability of COOH-MWCNTs in NaCl solutions,[5] which was attributed to the loss of carboxyl groups as shown in Figure 1. Figure 7a presents the sedimentation curves of COOH-MWCNTs after reacting with •OH for various period of time. The initial COOH-MWCNTs were very stable in 10 mM NaCl due to their highly negatively charged surfaces. The stability of COOH-MWCNTs gradually decreased with increasing reaction time with •OH. This decrease in stability is consistent with the change in

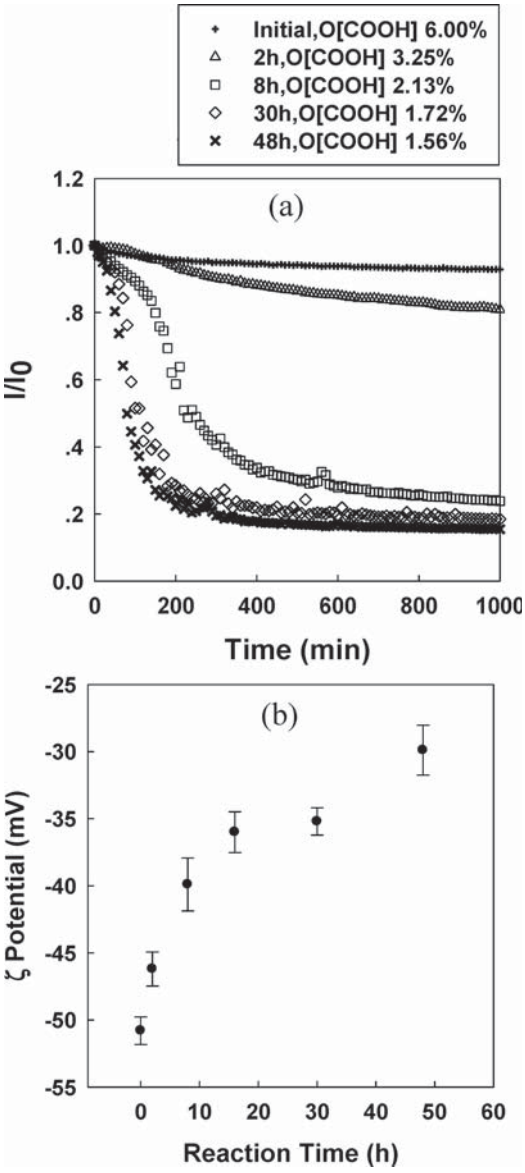

Figure 7. Sedimentation curves of COOH-MWCNTs with different reaction time with •OH in 10 mM NaCl solutions (a) and the ζ potential of COOH-MWCNTs as a function of reaction time with •OH in 1 mM NaCl solutions (b). The atomic oxygen concentration associated with carboxyl groups, O[COOH], for each sample was provided in the legend. Error bars represent standard deviation.

surface ζ potential (Figure 7b). Reactions with •OH reduced the negative surface ζ potential of COOH-MWCNTs, leading to weaker electrostatic repulsion and hence faster aggregation and sedimentation. To better understand the role of surface functionality in COOH-MWCNT mobility, the relationships between O[Total] or individual functional groups and the stability were examined. Pristine MWCNTs and MWCNTs with low O[Total] were known to be unstable in aqueous phase and the stability of MWCNTs can be improved by increasing O[Total].[43,44] However, the stability of COOH-MWCNTs did not correlate well with the O[Total]. It continued to decrease after 11 h of reaction, when O[Total] remained stable. On the other hand, a good correlation was found between the O[COOH] and the stability of COOH-MWCNTs (Figure 7a and Supporting Information Figure S4). Considering that carboxyl groups are the main oxygen-containing functional groups that dissociate at the experiment pH, they are expected to be the major factor that controls the surface charge and the stability of COOH-MWCNTs. The results agree with our previous study of COOH-MWCNT stability before and after UVA irradiation[23] as well as earlier studies examining the influence of surface functionality on the stability of acid modified MWCNTs.[43,45] The change of surface oxygen-containing functional groups is also expected to influence the interactions between COOH-MWCNTs and natural organic matter[46] which is reported to strongly stabilize MWCNTs through steric repulsion.[46,47] These results highlight the important role of ROS-mediated transformation of COOH-MWCNTs in their environmental transport. On the other hand, aggregation of fullerenes was found to significantly inhibit their ability to generate ROS in UVA light due to self-quenching.[8,9] Destabilization of COOH-MWCNTs during ROS-mediated transformation may also lead to reduced photoactivity.

Environmental Implication. This investigation reveals that COOH-MWCNTs undergo photochemical transformation at significant rates under UVA irradiation at intensity similar to that in sunlight. Thus COOH-MWCNTs are expected to be reactive and their surface chemistry is dynamic in natural aquatic systems. Such dynamic transformation is expected to have significant implications for CNT fate and transport modeling and risk assessment. The photochemical transformation processes are mediated by ROS. In natural aquatic environments, ROS can be generated by nitrite and nitrate photolysis, natural organic matter photosensitization and photo-Fenton reactions. Interactions between CNTs and these ROS generation processes and their importance relative to ROS photogeneration by CNTs themselves need further investigation. Findings from this study also provide some insight on the fate of CNTs in advanced oxidation processes for water treatment. For instance, the $[^{\bullet}OH]_{ss}$ in the H_2O_2/UVC process is usually orders of magnitude higher than the $[^{\bullet}OH]_{ss}$ generated by the H_2O_2/UVA process used in this study. CNTs in the water/wastewater stream are therefore expected to be oxidized or even mineralized during the H_2O_2/UVC process.

■ ASSOCIATED CONTENT

Ⓢ Supporting Information

Details of the calculation of ROS steady state concentration, the chemical derivatization vessel, the surface oxygen and nitrogen concentrations of COOH-MWCNTs after L-histidine inhibition experiments, the mineralization of COOH-MWCNTs under UVA light, and the stability of COOH-MWCNTs quantified by $t_{0.9}$ as a function of the O[COOH] can be found in the Supporting Information. This material is available free of charge via Internet at http://pubs.acs.org/.

■ AUTHOR INFORMATION

Corresponding Author

*Phone: (713)348-2046. Fax: (713)348-5268. E-mail: qilin.li@rice.edu.

Notes

The authors declare no competing financial interest.

■ ACKNOWLEDGMENTS

This work was supported by the USEPA STAR program (Grant no. R834093). Its contents are solely the responsibility of the grantee and do not necessarily represent the official views of the

USEPA. Further, USEPA does not endorse the purchase of any commercial products or services mentioned in the publication. We thank Jonathon A. Brame and Mengyan Li for assisting the HPLC measurements. We also thank Professors Mingce Long, R. Bruce Weisman and Howard Fairbrother for the helpful discussions.

REFERENCES

(1) De Volder, M. F.; Tawfick, S. H.; Baughman, R. H.; Hart, A. J. Carbon Nanotubes: Present and Future Commercial Applications. *Science* **2013**, *339* (6119), 535−539.

(2) Kotchey, G. P.; Hasan, S. A.; Kapralov, A. A.; Ha, S. H.; Kim, K.; Shvedova, A. A.; Kagan, V. E.; Star, A. A Natural Vanishing Act: The Enzyme-Catalyzed Degradation of Carbon Nanomaterials. *Acc. Chem. Res.* **2012**, *45* (10), 1770−1781.

(3) Allen, B. L.; Kotchey, G. P.; Chen, Y. N.; Yanamala, N. V. K.; Klein-Seetharaman, J.; Kagan, V. E.; Star, A. Mechanistic Investigations of Horseradish Peroxidase-Catalyzed Degradation of Single-Walled Carbon Nanotubes. *J. Am. Chem. Soc.* **2009**, *131* (47), 17194−17205.

(4) Zhao, Y.; Allen, B. L.; Star, A. Enzymatic Degradation of Multiwalled Carbon Nanotubes. *J. Phys. Chem. A* **2011**, *115* (34), 9536−9544.

(5) Hwang, Y. S.; Qu, X.; Li, Q. The Role of Photochemical Transformations in the Aggregation and Deposition of Carboxylated Multiwall Carbon Nanotubes Suspended in Water. *Carbon* **2013**, *55*, 81−89.

(6) Hou, W. C.; Jafvert, C. T. Photochemical Transformation of Aqueous C-60 Clusters in Sunlight. *Environ. Sci. Technol.* **2009**, *43* (2), 362−367.

(7) Hou, W. C.; Kong, L. J.; Wepasnick, K. A.; Zepp, R. G.; Fairbrother, D. H.; Jafvert, C. T. Photochemistry of Aqueous C-60 Clusters: Wavelength Dependency and Product Characterization. *Environ. Sci. Technol.* **2010**, *44* (21), 8121−8127.

(8) Lee, J.; Fortner, J. D.; Hughes, J. B.; Kim, J. H. Photochemical Production of Reactive Oxygen Species by C-60 in the Aqueous Phase during UV Irradiation. *Environ. Sci. Technol.* **2007**, *41* (7), 2529−2535.

(9) Lee, J.; Kim, J. H. Effect of Encapsulating Agents on Dispersion Status and Photochemical Reactivity of C-60 in the Aqueous Phase. *Environ. Sci. Technol.* **2008**, *42* (5), 1552−1557.

(10) Hwang, Y. S.; Li, Q. L. Characterizing Photochemical Transformation of Aqueous *n*C(60) under Environmentally Relevant Conditions. *Environ. Sci. Technol.* **2010**, *44* (8), 3008−3013.

(11) Kong, L. J.; Tedrow, O.; Chan, Y. F.; Zepp, R. G. Light-Initiated Transformations of Fullerenol in Aqueous Media. *Environ. Sci. Technol.* **2009**, *43* (24), 9155−9160.

(12) Matsumoto, Y.; Koinuma, M.; Ida, S.; Hayami, S.; Taniguchi, T.; Hatakeyama, K.; Tateishi, H.; Watanabe, Y.; Amano, S. Photoreaction of Graphene Oxide Nanosheets in Water. *J. Phys. Chem. C* **2011**, *115* (39), 19280−19286.

(13) Chen, C. Y.; Jafvert, C. T. The Role of Surface Functionalization in the Solar Light-Induced Production of Reactive Oxygen Species by Single-Walled Carbon Nanotubes in Water. *Carbon* **2011**, *49* (15), 5099−5106.

(14) Joshi, A.; Punyani, S.; Bale, S. S.; Yang, H. C.; Borca-Tasciuc, T.; Kane, R. S. Nanotube-Assisted Protein Deactivation. *Nat. Nanotechnol.* **2008**, *3* (1), 41−45.

(15) Haag, W. R.; Hoigne, J.; Gassman, E.; Braun, A. M. Singlet Oxygen in Surface Waters 0.1. Furfuryl Alcohol As a Trapping Agent. *Chemosphere* **1984**, *13* (5−6), 631−640.

(16) Maurette, M. T.; Oliveros, E.; Infelta, P. P.; Ramsteiner, K.; Braun, A. M. Singlet Oxygen and Superoxide—Experimental Differentiation and Analysis. *Helv. Chim. Acta* **1983**, *66* (2), 722−733.

(17) Chen, C. Y.; Jafvert, C. T. Photoreactivity of Carboxylated Single-Walled Carbon Nanotubes in Sunlight: Reactive Oxygen Species Production in Water. *Environ. Sci. Technol.* **2010**, *44* (17), 6674−6679.

(18) Sutherland, M. W.; Learmonth, B. A. The Tetrazolium Dyes MTS and XTT Provide New Quantitative Assays for Superoxide and Superoxide Dismutase. *Free Radical Res.* **1997**, *27* (3), 283−289.

(19) Ishibashi, K.; Fujishima, A.; Watanabe, T.; Hashimoto, K. Detection of Active Oxidative Species in TiO_2 Photocatalysis Using the Fluorescence Technique. *Electrochem. Commun.* **2000**, *2* (3), 207−210.

(20) Ishibashi, K.; Fujishima, A.; Watanabe, T.; Hashimoto, K. Quantum Yields of Active Oxidative Species Formed on TiO_2 Photocatalyst. *J. Photochem. Photobiol., A* **2000**, *134* (1−2), 139−142.

(21) Wepasnick, K. A.; Smith, B. A.; Schrote, K. E.; Wilson, H. K.; Diegelmann, S. R.; Fairbrother, D. H. Surface and Structural Characterization of Multi-Walled Carbon Nanotubes Following Different Oxidative Treatments. *Carbon* **2011**, *49* (1), 24−36.

(22) Langley, L. A.; Villanueva, D. E.; Fairbrother, D. H. Quantification of Surface Oxides on Carbonaceous Materials. *Chem. Mater.* **2006**, *18* (1), 169−178.

(23) Hwang, Y. S.; Qu, X. L.; Li, Q. L. The Role of Photochemical Transformations in the Aggregation and Deposition of Carboxylated Multiwall Carbon Nanotubes Suspended in Water. *Carbon* **2013**, *55*, 81−89.

(24) Latch, D. E.; McNeill, K. Microheterogeneity of Singlet Oxygen Distributions in Irradiated Humic Acid Solutions. *Science* **2006**, *311* (5768), 1743−1747.

(25) Hassett, J. P. Chemistry—Dissolved Natural Organic Matter As a Microreactor. *Science* **2006**, *311* (5768), 1723−1724.

(26) Wilkinson, F.; Helman, W. P.; Ross, A. B. Rate Constants for the Decay and Reactions of the Lowest Electronically Excited Singlet State of Molecular Oxygen in Solution. an Expanded and Revised Compilation. *J. Phys. Chem. Ref. Data* **1995**, *24* (2), 663 DOI: 10.1063/1.555965.

(27) Dickinson, B. C.; Chang, C. J. Chemistry and Biology of Reactive Oxygen Species in Signaling or Stress Responses. *Nat. Chem. Biol.* **2011**, *7* (8), 504−511.

(28) Grandbois, M.; Latch, D. E.; McNeill, K. Microheterogeneous Concentrations of Singlet Oxygen in Natural Organic Matter Isolate Solutions. *Environ. Sci. Technol.* **2008**, *42* (24), 9184−9190.

(29) Liao, Y.; Brame, J.; Que, W.; Xiu, Z.; Xie, H.; Li, Q.; Fabian, M.; Alvarez, P. J. Photocatalytic Generation of Multiple ROS Types Using Low-Temperature Crystallized Anodic TiO_2 Nanotube Arrays. *J. Hazard. Mater.* **2013**, *260*, 434−441.

(30) Alvarez, N. T.; Kittrell, C.; Schmidt, H. K.; Hauge, R. H.; Engel, P. S.; Tour, J. M. Selective Photochemical Functionalization of Surfactant-Dispersed Single Wall Carbon Nanotubes in Water. *J. Am. Chem. Soc.* **2008**, *130* (43), 14227−14233.

(31) Reber, J. F.; Meier, K. Photochemical Production of Hydrogen with Zinc-Sulfide Suspensions. *J. Phys. Chem.* **1984**, *88* (24), 5903−5913.

(32) Neta, P.; Huie, R. E. Free-Radical Chemistry of Sulfite. *Environ. Health Perspect.* **1985**, *64*, 209−217.

(33) Dukovic, G.; White, B. E.; Zhou, Z. Y.; Wang, F.; Jockusch, S.; Steigerwald, M. L.; Heinz, T. F.; Friesner, R. A.; Turro, N. J.; Brus, L. E. Reversible Surface Oxidation and Efficient Luminescence Quenching in Semiconductor Single-Wall Carbon Nanotubes. *J. Am. Chem. Soc.* **2004**, *126* (46), 15269−15276.

(34) Chan, S. P.; Chen, G.; Gong, X. G.; Liu, Z. F. Oxidation of Carbon Nanotubes by Singlet O-2. *Phys. Rev. Lett.* **2003**, *90* (8), No. 086403.

(35) Buxton, G. V.; Greenstock, C. L.; Helman, W. P.; Ross, A. B. Critical-Review of Rate Constants for Reactions of Hydrated Electrons, Hydrogen-Atoms and Hydroxyl Radicals ($^{\bullet}OH/O^{-}$) in Aqueous-Solution. *J. Phys. Chem. Ref. Data* **1988**, *17* (2), 513−886.

(36) Li, W.; Bai, Y.; Zhang, Y. K.; Sun, M. L.; Cheng, R. M.; Xu, X. C.; Chen, Y. W.; Mo, Y. J. Effect of Hydroxyl Radical on the Structure of Multi-walled Carbon Nanotubes. *Synth. Met.* **2005**, *155* (3), 509−515.

(37) Zhang, X. W.; Lei, L. C.; Xia, B.; Zhang, Y.; Fu, J. L. Oxidization of Carbon Nanotubes through Hydroxyl Radical Induced by Pulsed

O(2) Plasma and Its Application for O(2) Reduction in Electro-Fenton. *Electrochim. Acta* **2009**, *54* (10), 2810−2817.
(38) Graupner, R. Raman Spectroscopy of Covalently Functionalized Single-Wall Carbon Nanotubes. *J. Raman Spectrosc.* **2007**, *38* (6), 673−683.
(39) Salzmann, C. G.; Llewellyn, S. A.; Tobias, G.; Ward, M. A. H.; Huh, Y.; Green, M. L. H. The Role of Carboxylated Carbonaceous Fragments in the Functionalization and Spectroscopy of a Single-Walled Carbon-Nanotube Material. *Adv. Mater.* **2007**, *19* (6), 883−887.
(40) Simmons, J. M.; Nichols, B. M.; Baker, S. E.; Marcus, M. S.; Castellini, O. M.; Lee, C. S.; Hamers, R. J.; Eriksson, M. A. Effect of Ozone Oxidation on Single-Walled Carbon Nanotubes. *J. Phys. Chem. B* **2006**, *110* (14), 7113−7118.
(41) Qui, N. V.; Scholz, P.; Krech, T.; Keller, T. F.; Pollok, K.; Ondruschka, B. Multiwalled Carbon Nanotubes Oxidized by UV/H(2)O(2) as Catalyst for Oxidative Dehydrogenation of Ethylbenzene. *Catal. Commun.* **2011**, *12* (6), 464−469.
(42) Martinez, M. T.; Callejas, M. A.; Benito, A. M.; Cochet, M.; Seeger, T.; Anson, A.; Schreiber, J.; Gordon, C.; Marhic, C.; Chauvet, O.; Fierro, J. L. G.; Maser, W. K. Sensitivity of Single-Wall Carbon Nanotubes to Oxidative Processing: Structural Modification, Intercalation and Functionalisation. *Carbon* **2003**, *41* (12), 2247−2256.
(43) Smith, B.; Wepasnick, K.; Schrote, K. E.; Cho, H. H.; Ball, W. P.; Fairbrother, D. H. Influence of Surface Oxides on the Colloidal Stability of Multi-Walled Carbon Nanotubes: A Structure-Property Relationship. *Langmuir* **2009**, *25* (17), 9767−9776.
(44) Yi, P.; Chen, K. L. Influence of Surface Oxidation on the Aggregation and Deposition Kinetics of Multiwalled Carbon Nanotubes in Monovalent and Divalent Electrolytes. *Langmuir* **2011**, *27* (7), 3588−3599.
(45) Smith, B.; Wepasnick, K.; Schrote, K. E.; Bertele, A. H.; Ball, W. P.; O'Melia, C.; Fairbrother, D. H. Colloidal Properties of Aqueous Suspensions of Acid-Treated, Multi-Walled Carbon Nanotubes. *Environ. Sci. Technol.* **2009**, *43* (3), 819−825.
(46) Smith, B.; Yang, J.; Bitter, J. L.; Ball, W. P.; Fairbrother, D. H. Influence of Surface Oxygen on the Interactions of Carbon Nanotubes with Natural Organic Matter. *Environ. Sci. Technol.* **2012**, *46* (23), 12839−12847.
(47) Saleh, N. B.; Pfefferle, L. D.; Elimelech, M. Influence of Biomacromolecules and Humic Acid on the Aggregation Kinetics of Single-Walled Carbon Nanotubes. *Environ. Sci. Technol.* **2010**, *44* (7), 2412−2418.